*Proc. Int. Symp. Biomol. Struct. Interactions, Suppl. J. Biosci.,*
Vol. 8, Nos 3 & 4, August 1985, pp. 507-516. © Printed in India.

# Polymorphism in B-DNA: X-ray diffraction studies on Li-DNA fibres

P. PARRACK, M. SUNDARAMOORTHY AND V. SASISEKHARAN*
Molecular Biophysics Unit, Indian Institute of Science, Bangalore 560012, India

**Abstract.** From X-ray diffraction studies it is generally believed that B-DNA has the structural parameters n = 10 and h = 3·4 Å. However, for the first time we report that polymorphism in the B-form can be observed in DNA fibres. This was achieved by the precise control of salt and humidity in fibres and by the application of the precession method of X-ray diffraction to DNA fibres. The significant result obtained is that n = 10 is not observed for crystalline fibre patterns. In fact, n = 10 and h = 3·4 Å are not found to occur simultaneously. Instead, a range of values, n = 9·6–10·0 and h = 3·35 Å–3·41 Å is observed.

**Keywords.** Polymorphism; B-DNA; fibre diffraction.

## Introduction

The biologically important polymorphous form of DNA, the B-DNA, is believed to have a uniform double helical structure in the solid state with the number of residues per turn n = 10 and height per residue, h = 3·4 Å. These values for the B-form were obtained from models built to explain the crystalline X-ray diffraction patterns of the lithium salt of DNA (Langridge *et al.*, 1960; Arnott, 1970).

Even during the early days of DNA fibre diffraction analysis, it was recognised that the environment of DNA molecules in a fibre (salt type, its concentration and relative humidity, r.h.) influences its structure, giving rise to polymorphism (Langridge *et al.*, 1960). However, the exact control of salt (Li) concentration in fibres was achieved only recently (Parrack *et al.*, 1984). Detailed study of X-ray patterns of calf-thymus DNA at different amounts of lithium salt and at various humidities showed that (a) the X-ray patterns cannot be fully explained by uniform tenfold helical models for B-DNA, and (b) fine variations in salt and humidity cause the structure in the B-form to undergo transitions, even in the solid state (Parrack *et al.*, 1984; Dutta *et al.*, 1984).

The above results are in agreement with the findings from several other experiments. For example, solution studies have shown values of n = 10·4, 10·6 (Wang, 1979; Rhodes and Klug, 1980) as also a structural polymorphism within the B-form (Drew and Travers, 1984; Keene and Elgin, 1984). Even in the solid state, the nonuniform nature of the structure has been indicated from the crystal of the oligonucleotide d(CGCGAATTCGCG) (Dickerson and Drew, 1981) and from $^{31}$P NMR studies of fibres of natural DNA (Shindo *et al.*, 1980, 1984). Fibre studies of natural DNA in the presence of many organic solvents had been done by Zimmerman and Pheiffer (1980). They showed that the B-DNA structure could adopt several variants:

* To whom correspondence should be addressed.

n = 9·6 to n = 10·3 was observed for B-DNA, depending upon the type and amount of organic solvent, in addition to the nature and amount of salt. Thus, the variability and nonuniformity in the B-DNA structure have been well established during the last five years.

It is generally believed that fibre diffraction can give only average values of the structure. The humidity- and organic solvent-induced variations were detected by Zimmerman from paracrystalline X-ray patterns. However, exact control of salt, coupled with the precession method to DNA fibres enabled us to demonstrate for the first time that very fine structural variations can be quantitatively detected from well-defined crystalline X-ray patterns. Application of the precession method to fibres significantly improves the analysis of the fibre data. The observed variations again point out the enormous flexibility inherent in the DNA structure, proposed earlier from theoretical studies (Gupta *et al.*, 1980).

Here, we present the n and h values that have been obtained from precession photographs of lithium B-DNA at precisely known conditions of salt and humidity.

## Materials and methods

Fibres were prepared from calf thymus DNA (Sigma), as described before (Parrack *et al.*, 1984). The salt concentration in the fibres is expressed by $\Delta = (Li^+)/(DNA)$, the DNA concentration being measured in units of base-phosphates. Precession photographs were taken by perfectly aligning the fibre axis normal to the beam, and by using a zero-level screen. The flat-plate photograph of a fibre corresponds to the rotation photograph of a single crystal, and the precession photograph corresponds to that of the zero-level precession of a crystal rotated about a crystal axis. For such a precession photograph, a one-to-one correspondence between the reciprocal lattice points and reflections on the film are not obtained. Nevertheless, there is a linear correlation between these, leading to a limited but significant improvement in the analysis of the DNA fibre diffraction patterns. Details of this method will be discussed elsewhere (Sundaramoorthy, M., Parrack, P. and Sasisekharan, V., unpublished results). Suffice it to mention that helical parameters 'n' and 'h', as also the *C*-axis repeat, can be calculated from the precession photograph using the simple relations $n = d_{10}/d_1$, $h = d_{10}$ and $C = d_1$ where $d_{10}$ and $d_1$ denote the spacings of the tenth and first layer lines respectively. This makes it possible to calculate the parameters without referring to the geometry of the camera arrangement. A specimen to film distance D = 10 cm was used, greatly increasing the sensitivity of our measurements. Densitometric tracings were obtained from X-ray negatives using a Joyce-Loebl microdensitometer. Humidity in fibres was controlled by enclosing the fibre in a Lindemann capillary tube, containing a suitable saturated salt solution.

## Results and discussion

Figure 1 shows a usual flat-plate diffraction photograph for B-DNA (figure 1a), together with a precession photograph (figure 1b). The following differences between the two photographs deserve mention: (a) layer lines in figure 1b are straight and

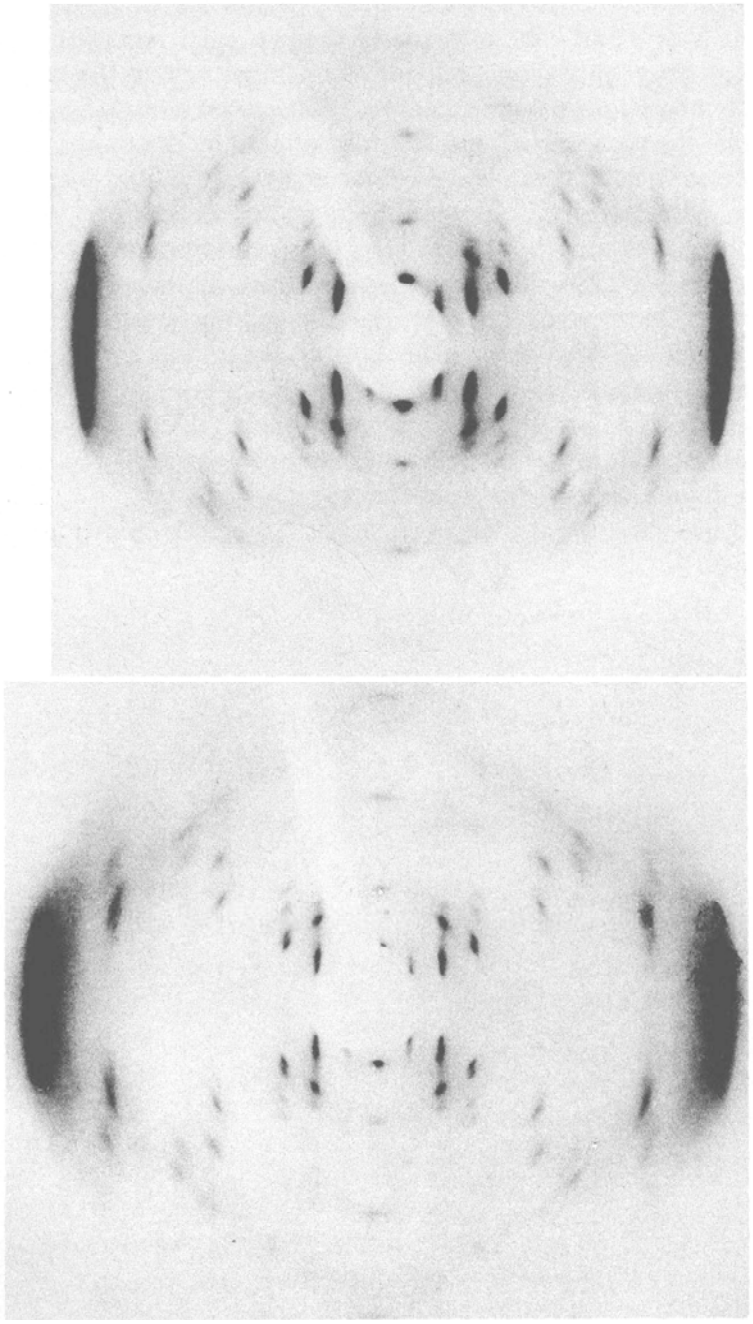

(a) (b)

**Figure 1.** (a) A flat-plate and (b) a precession X-ray diffraction photograph for Li-B DNA at r.h. = 66% and $\Delta = 1{\cdot}6$.

parallel, in contrast to those in figure la, and (b) even the higher order layers are obtained as sharp reflections in figure 1b, since the precession motion causes the fibre to be correctly tilted for each layer line. The above features for the precession method make this method suitable to measure accurately the values of n, h and *C*. As mentioned earlier, the linear correlation gives rise to the linear relation $d = \lambda D/\zeta$. Here $\lambda$ denotes the wave length of X-rays and $\zeta$ the ordinate of the particular reflection on the film. Thus $n = \zeta_{10} / \zeta_{1}$, a remarkably simple relation. Remembering that the layer lines are straight in a precession pattern, $\zeta$ is constant for reflections on a single layer line, and it is easy to appreciate the convenience and accuracy offered by the precession method.

Earlier, we detected structural variations characterised by qualitative changes in the diffraction pattern, namely, changes in crystallinity and in the intensity of meridional reflections appearing at the sixth and fourth layer lines in addition to that on the tenth layer line (Parrack *et al.*, 1984). The precession method allows us to quantify the variations in terms of the values of the helical parameters. The results are presented in table 1.

The precession photograph of the fibre at high humidity (98% r.h.) on which measurements were made to obtain the values given in the table, is shown in figure 2. The interesting point to note is that the generally accepted values n = 10 and h = 3·4 Å are not obtained simultaneously, from any photograph. For 66 % r.h., h ≃ 3·4 Å is obtained, but n is less than 10. On the other hand, the high humidity pattern gives n = 10, but h = 3·35 Å.

**Figure 2.** A precession X-ray diffraction photograph of the same fibre at high humidity (Δ = 1·6, r.h. = 98 %). This gives n = 10 and h = 3·35 Å (see text).

It must be remembered that the above values for helical parameters are obtained under the assumption that the structure can be approximated to a regular helical one. The meridional reflection on the sixth layer seen in figure 1b provides a reason to believe that the structure is not truly helical. A weaker meridional reflection on the fourth layer (not clearly seen in figure 1b) supports this belief (discussed in more detail in Dutta *et al.,* 1984). However, the present data do not allow us to arrive at the precise deviations from a helical nature that could give rise to such meridional reflections. Therefore, we speak of 'helical parameters' only in a restricted sense, throughout this report. Figures 3 and 4 schematically depict the essence of our observations: structural variability and nonhelical nature.

The synergistic effects of salt and humidity on helical parameters can be noticed from table 1. The values of all the parameters undergo gradual changes and a range in 'n' from 9·6–10·0 is found. However, mention must be made of another possibility: 'n' can be greater instead of being less than ten. The values of 'n' have been shown to be less than ten because the so-called tenth layer line has been assumed to contain a meridional *(i.e.* $J_0$*)* reflection. But it has been already observed that this may not be true in general (Parrack *et al.,* 1984). Low exposure flat-plate diffraction patterns with the fibre tilted for the tenth layer lead us to another possibility: the tenth layer is due to Bessel function $J_{-1}$ instead of $J_0$. Figures 5 and 6 show the tenth layer lines for $\Delta = 1{\cdot}4$ and $\Delta = 1{\cdot}6$ respectively, alongwith densitometric tracings taken along the layer. The meridional

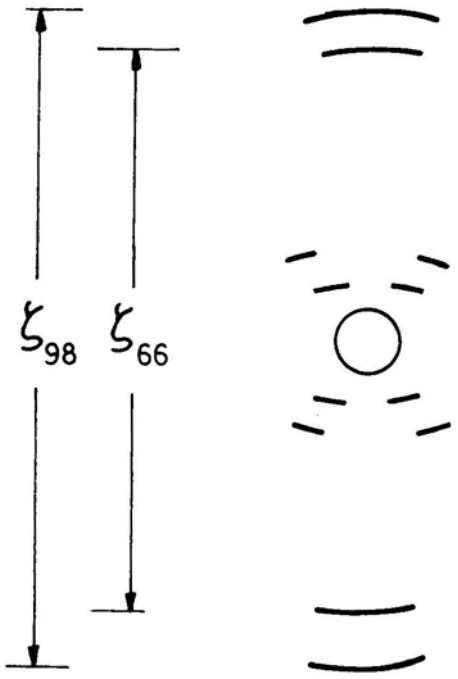


**Figure 3.** A schematic diagram to show the change in the tenth layer spacing when r.h. is raised. Only the first, second and tenth layers are shown. Suffixes denote r.h. values. $\zeta_{98} > \zeta_{66}$, which leads to $d_{98}$ (3·35 Å) < $d_{66}$ (3·4 Å).

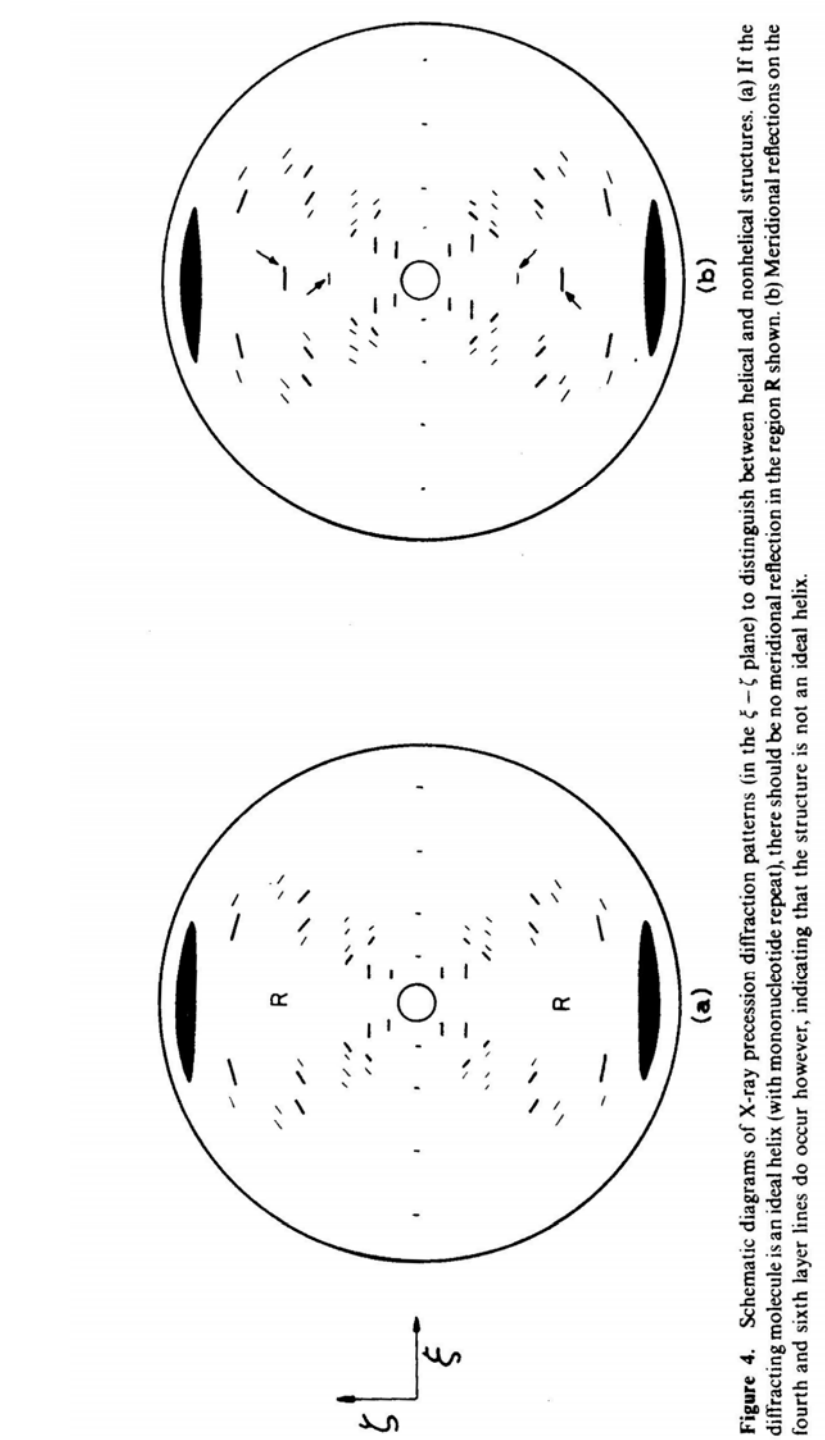


**Figure 4.** Schematic diagrams of X-ray precession diffraction patterns (in the $\xi - \zeta$ plane) to distinguish between helical and nonhelical structures. (a) If the diffracting molecule is an ideal helix (with mononucleotide repeat), there should be no meridional reflection in the region R shown. (b) Meridional reflections on the fourth and sixth layer lines do occur however, indicating that the structure is not an ideal helix.

**Table 1.** Values of structural parameters for different salts and humidities.

| Δ | r.h. | h(Å) | $C$(Å) | $n$ |
|---|---|---|---|---|
| 1·4 | 66% | 3·41 | 32·72 | 9·6 |
| 1·6 | 66% | 3·39 | 32·98 | 9·7 |
| 1·6 | 98% | 3·35 | 33·50 | 10·0 |

Measurements for h are accurate upto ± 0·005 Å for 66% r.h., and upto ± 0·01 Å for 98 % r.h. These results are based on the assumption that the tenth layer line is due to $J_0$. Instead, if it is due to $J_{-1}$ (see Parrack *et al.*, 1984), this would result in values of $n > 10$ for r.h. = 66%, rather than $n < 10$.

reflection is absent for Δ = 1·4 and present for Δ = 1·6. Two off-meridional reflections, which could be due to Bessel order −1, are also present for both the salt concentrations. If we consider the tenth layer meridian of figure 6 (Δ = 1·6) on the same footing as the meridional reflections on fourth and sixth layer lines; *i.e.*, they are due to nonhelical features in the structure, then the tenth layer could be due to $J_{-1}$. The off-meridional reflections on the tenth layer seem to have the same $\xi$ values as non-meridional reflections on the second layer, as can be seen from figure 7. To be in a position to offer an explanation for the appearance and disappearance of the tenth layer meridian with a slight change in salt concentration and also to choose between $J_0$ and $J_{-1}$ for the tenth layer, the reflections need to be correctly indexed. This can be done conveniently from precession photographs and work is in progress in our laboratory in this direction.

Fibre diffraction studies of DNA is now more than thirty years old. But still, when we started to systematically investigate the exact conditions necessary for good fibres which would give highly crystalline patterns, it became apparent that so much still remained to be done and that X-ray fibre patterns contain such a lot of unexplained data. Polymorphism within the B-form reemphasises the dynamic nature of the DNA structure and demonstrates the flexibility present in DNA: it can undergo minute structural changes with a slightly different environment. In the literature, there is a tendency to compare different solution data (IR, NMR, etc.) with existing DNA models. These models, obtained from X-ray studies, now seem to be only approximate and thus, grossly inadequate for such detailed comparisons using precise coordinates. Likewise, refinement of helical models for B-DNA also loses its value. Hopefully, with the introduction of the precession method to fibre diffraction, we might be able to find out the extent of variability in B-DNA, *i. e.* the range of n and h values which give rise to the B-type X-ray patterns.

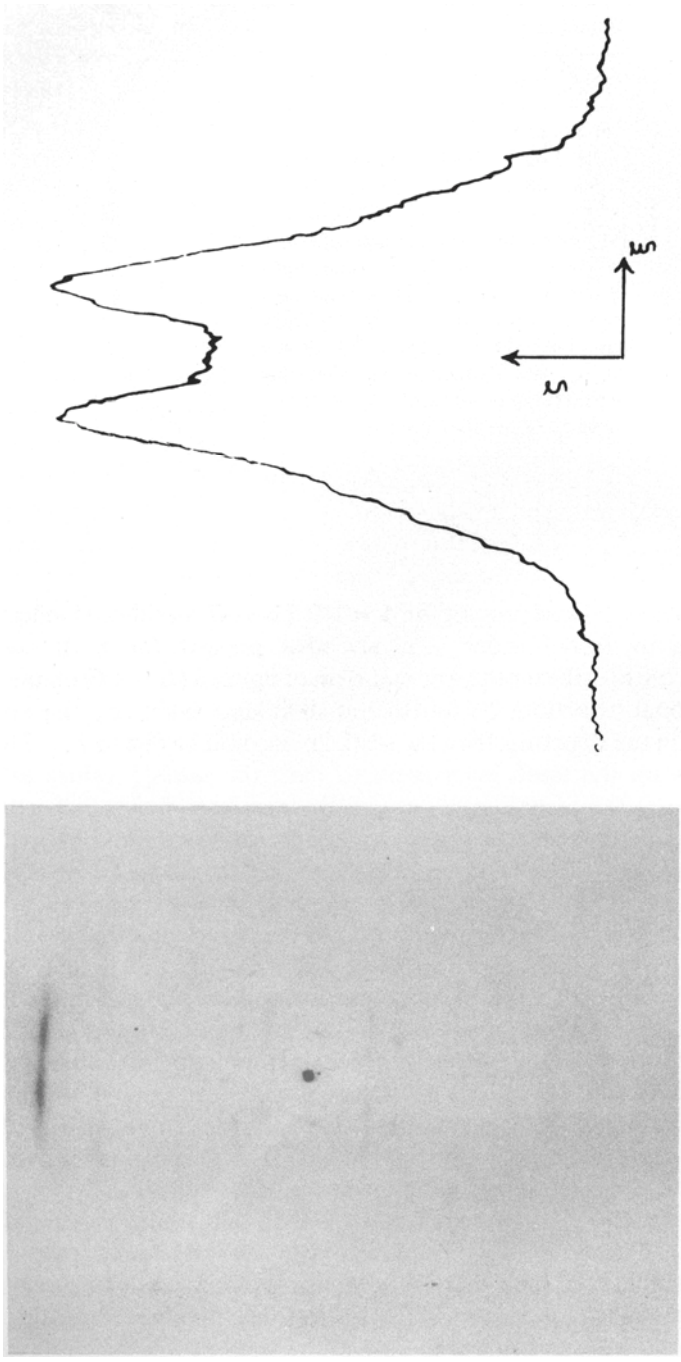


**Figure 5.** (a) A flat plate X-ray diffraction photograph for Li-B DNA with $\Delta = 1{\cdot}4$ and r.h. 66% to show the fine structure of the tenth layer (see text). The fibre was tilted for the tenth layer and the pattern recorded with low exposure time. There is no meridian on the tenth layer and only two off-meridional reflections are seen, as a doublet. (b) The densitometer tracing of the tenth layer line of the above photograph. $\xi - \zeta$ axes are shown.

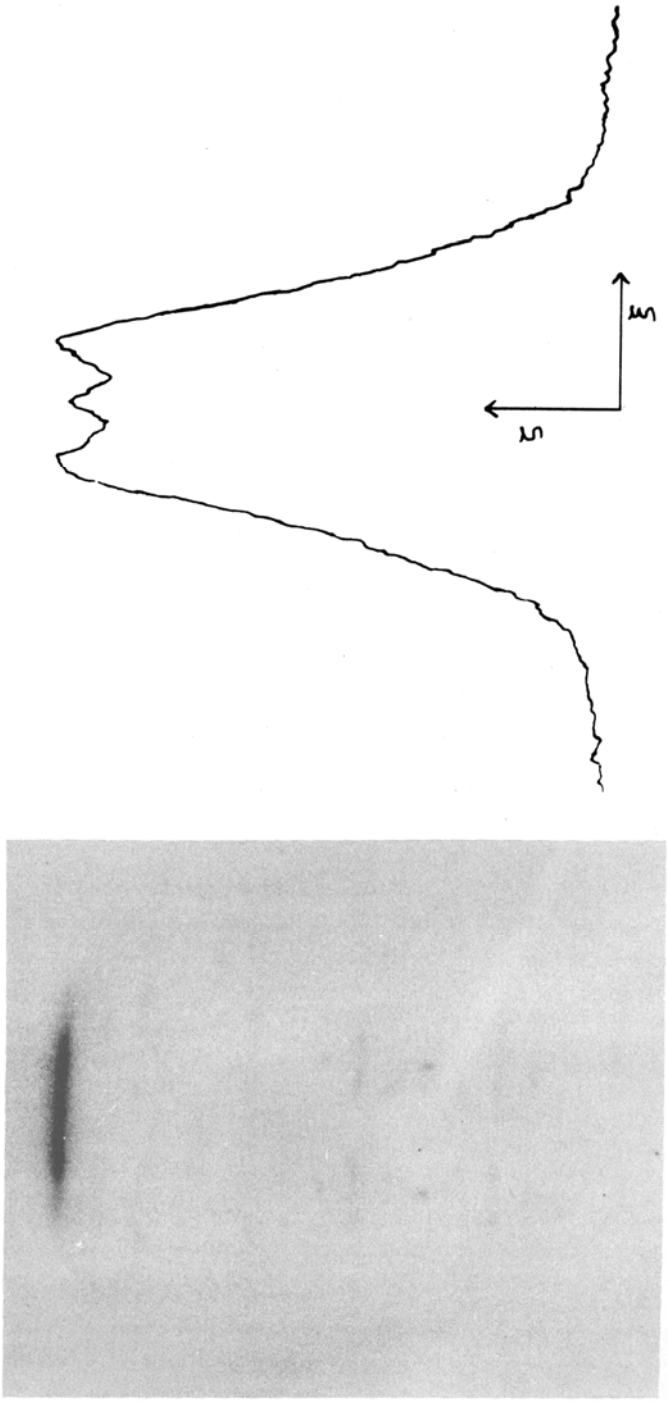


**Figure 6.** (a) A similar flat plate photograph as in figure 5a, but with $\Delta = 1{\cdot}6$. There is a meridian on the tenth layer which was not there in figure 5. Here, the two off-meridional reflections of figure 5 are also seen alongwith this meridian, as a triplet.

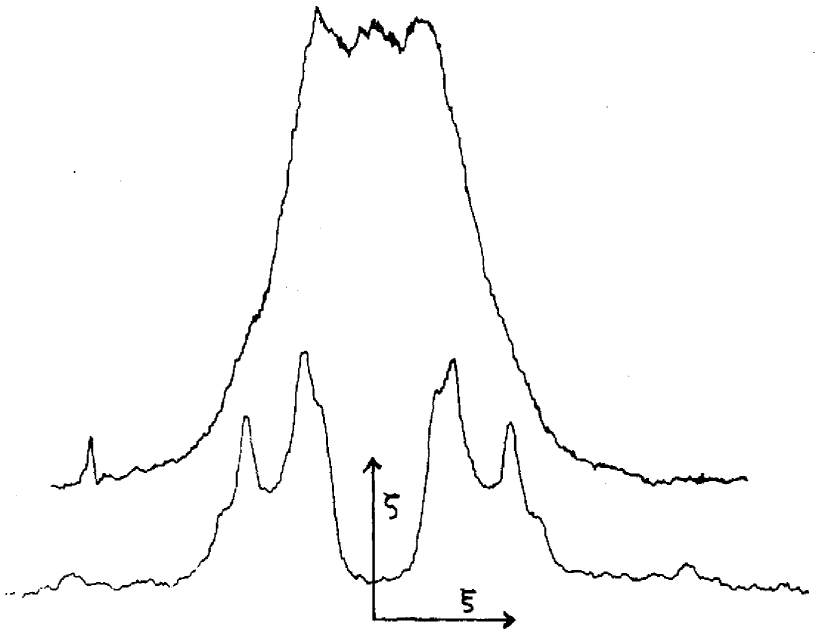


**Figure 7.** Densitometer tracings of the precession X-ray diffraction photograph shown in figure 1b, taken for the second and tenth layer lines. Note that the off-meridional reflections on the second and the tenth layer lines have the same reciprocal ($\xi$) values.

## Acknowledgement

This work was partially supported by the DST-SERC grant under the Thrust Area Programme of the Government of India (Scheme No. DST/MBU/VS: 64).

## References

Arnott, S. (1970) in *Progress in Biophysics and Molecular Biology* (eds J. A. V. Butler and D. Noble) (Oxford: Pergamon Press) Vol. 21, p. 265.
Dickerson, R. E. and Drew, H. R. (1981) *J. Mol. Biol.*, **149,** 761.
Drew, H. R. and Travers, A. A. (1984) *Cell*, **37,** 491.
Dutta, S., Parrack, P. and Sasisekharan, V. (1984) *FEBS Lett.*, **176,** 110.
Gupta, G., Bansal, M. and Sasisekharan, V. (1980) *Int. J. Biol. Macromol.*, **2,** 368.
Keene, M. A. and Elgin, S. C. R. (1984) *Cell*, **36,** 121.
Langridge, R., Wilson, H. R., Hooper, C. W., Wilkins, M. H. F. and Hamilton, L. D. (1960) *J. Mol. Biol.*, **2,**19.
Parrack, P., Dutta, S. and Sasisekharan, V. (1984) *J. Biomol. Struct. Dynam.*, **2,** 149.
Rhodes, D. and Klug, A. (1980) *Nature* (*London*)*,* **286,** 573.
Shindo, H., Wooten, J. B., Pheiffer, B. H. and Zimmerman, S. B. (1980) *Biochemistry*, **19,** 518.
Shindo, H., Fujiwara, T., Akutsu, H., Matsumoto, U. and Shimidzu, M. (1984) *J. Mol. Biol.*, **74,** 221.
Wang, J. C. (1979) *Proc. Natl. Acad. Sci. USA*, **76,** 200.
Zimmerman, S. B. and Pheiffer, B. H. (1980) *J. Mol. Biol.*, **142,** 315.